

Phonon-induced pure dephasing in exciton-biexciton quantum dot systems driven by ultrafast laser pulse sequences

V. M. Axt and T. Kuhn

Institut für Festkörperteorie, Westfälische Wilhelms-Universität Münster, Wilhelm-Klemm-Strasse 10, 48149 Münster, Germany

A. Vagov and F. M. Peeters

Department of Physics, University of Antwerpen, Groenenborgerlaan 171, 2020 Antwerpen, Belgium

(Received 19 May 2005; revised manuscript received 5 July 2005; published 8 September 2005)

A semiconductor quantum dot model accounting for single exciton as well as biexciton states coupled to phonons and laser light is investigated in the limit of strong electronic confinement. For an arbitrary sequence of excitations with ultrafast pulses analytical solutions are obtained for all density-matrix elements. The results are nonperturbative with respect to both the carrier-phonon and the carrier-light coupling. Numerical results for a single pulse excitation are presented illustrating spectral features of our solution as well as pulse area and temperature dependences.

DOI: [10.1103/PhysRevB.72.125309](https://doi.org/10.1103/PhysRevB.72.125309)

PACS number(s): 78.67.Hc, 78.47.+p, 63.22.+m, 63.20.Kr

I. INTRODUCTION

The most attractive property of semiconductor quantum dots (QDs) is their ability to provide adjustable discrete spectra.^{1,2} In neutral QDs these discrete energies correspond to single excitons and multiexciton complexes.^{3–9} Especially well studied are excitonic excitations^{10–18} but there is also a fastly growing literature on higher excitonic complexes.^{3–9} Among the latter a particular focus is on the properties of biexcitonic excitations^{3,7,19–33} including the characterization of biexciton binding energies in QDs,^{34–43} the LO phonon assisted biexciton generation,^{44,45} and measurements of biexcitonic coherences.⁴⁶ Biexcitonic dot states were proposed as a source of entangled or squeezed photons,^{25,47,48} which can be useful for quantum information processing devices. Also for many optical experiments it can be important to include biexcitonic effects even when it is justified to neglect transitions to higher excitonic states because of the energetic separation of the latter. In the absence of magnetic impurities and strong external magnetic fields the lowest exciton states are almost spin degenerate and, consequently, the biexciton state which comprises two excitons can be excited by applying a short laser pulse with a sufficiently broad spectrum. Early theoretical^{34,38} and experimental studies³⁷ have already demonstrated that the presence of biexcitonic states considerably affects nonlinear optical properties of QD systems. Advancing the optical methods towards the femtosecond time domain a growing number of experiments focussed on influences of biexcitonic QD states on the ultrafast dynamics^{28,49,50} such as biexcitonic beat phenomena in the four-wave-mixing (FWM) emission of QDs.^{51,52} Furthermore, it has even been proposed to use exciton-biexciton systems to implement quantum gate operations^{53–56} and recently a successful experimental realization of the latter has been reported.⁵⁷

A much discussed issue for both excitonic^{12,15,51,58–63} and biexcitonic transitions^{7,27–30} is decoherence. The interest in this subject is driven on the one hand, by the desire to suppress dephasing processes which provide a major obstacle

for all types of coherent applications and device operations. On the other hand, decoherence in QDs attracts attention because of its interesting physical properties which result from the discrete nature of the electronic states interacting with a solid state environment. In particular, so-called “pure dephasing” processes which do not lead to transitions between electronic states can become of utmost importance because in QD systems their effect is not so strongly masked by energy conserving transitions as in higher-dimensional systems. Indeed, comparing measurements with theory suggests that the initial decoherence of a QD excited by ultrafast pulses is clearly dominated by acoustic phonon induced pure dephasing.^{51,62–64} This initial dynamics is completed on a picosecond time scale followed by a relaxation due to processes which evolve on much longer time scales such as radiative decay,^{15,18,27} anharmonic phonon couplings,⁶⁵ or charge fluctuations in the surrounding environment.⁶⁶ Pure dephasing provides for a prototype of a genuine non-Markovian interaction because the conservation of single particle energies which is a necessary prerequisite of a Markovian theory is excluded here. The non-Markovian nature of pure dephasing manifests itself in unusual properties such as a nonmonotonous temperature dependence of the initial decay time^{63,64} or a nonexponential decay^{51,63,64} which is related to non-Lorentzian spectra^{12,61–63} that have recently been observed also for biexcitonic transitions.³⁰ A further characteristic of non-Markovian processes is the controllability of the decay by suitably shaped pulses which has been predicted theoretically.^{67,68}

Clearly, due to the nonexponential decay it is not possible to capture the essence of pure dephasing by a rate model where the electronic decoherence is accounted for by phenomenological decay rates. The key ingredient of the standard description of phonon-induced pure dephasing is the so-called independent Boson model.^{12,62,69} Although many analytical results are known for this model,^{70,71} exact solutions are usually not available when it is extended by a coupling between different electronic levels due to other mechanisms such as external laser fields. The latter is the relevant

model for the optically driven dynamics in QDs. It describes the nonlinear optical response including Rabi rotations as well as nonequilibrium phonons that are generated by the optical excitation process.⁶² Here, we are dealing with a special case of a spin-Boson type system that can only be treated approximately. Although there is no solution to this problem in general, we have shown recently that all elements of density matrix can be constructed in closed form provided the laser field consists of a sequence of ultrafast pulses and provided that the electronic degrees of freedom can be represented as an excitonic two-level system.⁶² These formulas allow one to perform exact calculations of the coherent nonlinear optical response of QDs relevant to ultrafast experiments where the laser excitation is shorter than the typical timescale of the phonon-induced dynamics. And indeed, corresponding experiments demonstrate that in the initial phase of the dynamics the pure dephasing theory provides for a quantitative description when standard material parameters are used.⁶⁴ The recent observation of phonon-induced sidebands in biexcitonic transitions³⁰ indicates that pure dephasing is a relevant process not only for excitonic but also for biexcitonic transitions. However, exact results for nonlinear optical signals—similar to the two-level case—have not yet been derived for the coupled exciton-biexciton system interacting with phonons and laser light. To the best of our knowledge, the calculations presented in Ref. 30 are so far the only known results dealing with effects of phonon-induced pure dephasing in the exciton-biexciton system of a QD. In these calculations luminescence spectra have been determined by evaluating the pertinent transition probabilities.

The aim of the present paper is to extend our previous results, that were restricted to electronic two-level systems, to the case where apart from the ground state we account for excitonic and biexcitonic states of a QD in the strong confinement limit. This limit is typically reached to a good approximation in self-assembled QDs.^{64,72} Included in our treatment are direct and exchange Coulomb interactions as well as the carrier-phonon coupling to an infinite number of phonon modes according to the independent Boson model and the dipole coupling to an external laser source. We shall show how to derive explicit exact formulas for all elements of the electronic and phononic density matrix relevant for an excitation by a sequence of ultrafast laser pulses. Technically, the ultrafast pulse regime is implemented by going over to the δ -pulse limit. Physically, this is the regime where the pulse durations are shorter than the time scale for the phonon-induced system dynamics. The quantitative agreement with experiments that has been found in Ref. 64 demonstrates the applicability of the δ -pulse limit to real experiments. As for the two-level case our results are nonperturbative with respect to both the carrier-phonon and the carrier-light coupling.

The paper is organized as follows. We start in Sec. II by introducing our model. In Sec. III we present the general analytical solution for all dynamical variables which is derived in Appendix A. Then the special case of a single pulse excitation is worked out in Sec. IV. This section is divided into several subsections where we discuss the specific properties of all electronic density matrix elements and some as-

pects related to optically generated nonequilibrium phonons. The paper closes with a summary of the main results and some concluding remarks.

II. FORMULATION OF THE MODEL

We account for a quantum dot with spin degenerate electronic single particle states coupled to phonons and laser light and interacting via the Coulomb interaction. The corresponding Hamiltonian can be written as

$$H = H_{\text{dot}} + H_{\text{phonon}} + H_{\text{dot-phonon}} + H_{\text{dot-light}}, \quad (1)$$

where H_{dot} describes the electronic structure of the dot and H_{phonon} represents the phonon energies. $H_{\text{dot-phonon}}$ accounts for the carrier-phonon and $H_{\text{dot-light}}$ for the carrier-light interaction.

We consider a quantum dot in the strong confinement limit, i.e., the electronic single particle states are energetically well separated and the Coulomb interaction provides negligible mixing between states with different single particle energies. From all confined quantum dot states we shall concentrate on the topmost valence band and the lowest conduction band states. To be specific we shall describe quantum dot electrons by the Fermion operators c_{σ} (c_{σ}^{\dagger}) which destroy (create) an electron with spin $\sigma = \uparrow$ or $\sigma = \downarrow$ in the lowest confined quantum dot orbital in the conduction band. Analogously we account for twofold degenerate dot states in the valence band. We shall assume that the topmost states are formed from degenerate heavy hole states which is typical, e.g., for GaAs type materials. A possible mixing with light hole states can usually be neglected in self-assembled QDs because the light hole states are energetically split from the heavy hole states by at least several tens of meV due to strain.¹⁴ In order to simplify the notation we denote the annihilation operator for the heavy hole state corresponding to an angular momentum component $m_j = 3/2$ ($m_j = -3/2$) by d_{\uparrow} (d_{\downarrow}) and the corresponding creation operator by d_{\uparrow}^{\dagger} (d_{\downarrow}^{\dagger}) where σ is either \uparrow or \downarrow . With this restriction H_{dot} can be written as $H_{\text{dot}} = H_{\text{band}} + H_{\text{Coulomb}}$, where

$$H_{\text{band}} = \frac{\hbar\Omega_0}{2} \sum_{\sigma} (c_{\sigma}^{\dagger}c_{\sigma} + d_{\sigma}^{\dagger}d_{\sigma}) \quad (2)$$

accounts for the single particle band energies, $\hbar\Omega_0$ denoting the gap energy, and

$$H_{\text{Coulomb}} = \frac{1}{2} \sum_{\sigma\sigma'} (V^{ee}c_{\sigma}^{\dagger}c_{\sigma}c_{\sigma'}^{\dagger}c_{\sigma'} + V^{hh}d_{\sigma}^{\dagger}d_{\sigma}d_{\sigma'}^{\dagger}d_{\sigma'} - 2V^{eh}c_{\sigma}^{\dagger}c_{\sigma}d_{\sigma'}^{\dagger}d_{\sigma'} + 2V_{\sigma\sigma'}^{\text{ex}}c_{\sigma}^{\dagger}d_{\sigma'}^{\dagger}d_{\sigma}c_{\sigma'}) \quad (3)$$

is the Coulomb interaction between the carriers in the dot. The four terms in Eq. (3) describe the repulsion between electrons and between holes, the electron-hole attraction, and the exchange interaction, respectively. The corresponding matrix elements V^{ee} , V^{hh} , V^{eh} , and $V_{\sigma\sigma'}^{\text{ex}}$ can be calculated from standard formulas once the single particle wave functions are known.⁷³⁻⁷⁵ For our present discussion a quantitative knowledge of these matrix elements is not required and thus they can be used as parameters.

Phonons will be represented by Boson operators b_ξ, b_ξ^\dagger , where ξ labels the phonon mode with energy $\hbar\omega_\xi$. The resulting contribution to the Hamiltonian reads

$$H_{\text{phonon}} = \sum_{\xi} \hbar\omega_{\xi} b_{\xi}^{\dagger} b_{\xi}. \quad (4)$$

The general derivation below is valid independent of the mode structure, i.e., one can consider any type of phonon mode and allow for arbitrary phonon spectra $\hbar\omega_{\xi}$.

The carrier-phonon coupling is treated in the standard form according to the Born-Oppenheimer approximation⁷⁶

$$H_{\text{dot phonon}} = \hbar \sum_{\xi\sigma} (g_{\xi}^e b_{\xi} c_{\sigma}^{\dagger} c_{\sigma} - g_{\xi}^h b_{\xi} d_{\sigma}^{\dagger} d_{\sigma} + \text{H.c.}), \quad (5)$$

where H.c. denotes the Hermitian conjugate and $g_{\xi}^e (g_{\xi}^h)$ are the carrier-phonon coupling matrix elements between an electron (hole) and the mode ξ which depend on the carrier wave functions, the phonon mode functions, as well as on the coupling mechanism.⁶¹ The most important coupling mechanisms for semiconductor structures are the deformation potential coupling to longitudinal acoustic (LA) phonons, the piezoelectric coupling to LA and transverse acoustic (TA) phonons, and the Fröhlich coupling to longitudinal optical (LO) phonons. All of these mechanisms can be accounted for in the form given by Eq. (5).

Finally, the dipole coupling to the light field reads in the rotating wave approximation

$$H_{\text{dot-light}} = -\mathbf{E}^* \cdot \hat{\mathbf{P}} + \text{H.c.}, \quad (6)$$

where the interband polarization of the dot is given by

$$\hat{\mathbf{P}} = M_0^* (d_{\downarrow} c_{\downarrow} \mathbf{e}_{\sigma^+} + d_{\uparrow} c_{\uparrow} \mathbf{e}_{\sigma^-}). \quad (7)$$

Here, M_0 is the dipole matrix element between valence and conduction band Bloch states and $\mathbf{e}_{\sigma^{\pm}}$ is the unit polarization vector with circular σ^{\pm} polarization. Equation (7) implements the usual selection rule that σ^+ (σ^-) light couples the $m_J = -3/2$ ($m_J = 3/2$) valence band to the spin down (up) conduction band state.

There are six independent neutral states in our restricted electronic space. The two dark exciton states $c_{\downarrow}^{\dagger} d_{\uparrow}^{\dagger} |0\rangle$ and $c_{\uparrow}^{\dagger} d_{\downarrow}^{\dagger} |0\rangle$ are not coupled by the Hamiltonian in Eq. (1) to other electronic states and will thus not be considered any further. The remaining four states $|0\rangle, |\sigma^+\rangle \equiv c_{\downarrow}^{\dagger} d_{\downarrow}^{\dagger} |0\rangle, |\sigma^-\rangle \equiv c_{\uparrow}^{\dagger} d_{\uparrow}^{\dagger} |0\rangle$, and $|B\rangle \equiv c_{\uparrow}^{\dagger} d_{\downarrow}^{\dagger} c_{\downarrow}^{\dagger} d_{\uparrow}^{\dagger} |0\rangle$ form the spin basis $|s\rangle$ of the dot. It turns out to be advantageous to rewrite the Hamiltonian (1) in the electronic eigenbasis, i.e., we introduce the eigenstates $|\nu\rangle$ of H_{dot} as new electronic basis states. The ground state $|0\rangle$ and the two-pair (biexciton) state $|B\rangle$ are already eigenstates of H_{dot} with the corresponding energies

$$\varepsilon_0 = 0, \quad (8a)$$

$$\varepsilon_B = 2(\hbar\Omega_0 + V^{ee} + V^{hh} - 2V^{eh}) + V_{\downarrow\downarrow}^{\text{ex}} + V_{\uparrow\uparrow}^{\text{ex}}. \quad (8b)$$

The diagonalization within the subspace of the single-pair states $|\sigma^{\pm}\rangle$ yields two states $|\pm\rangle$ with energies

$$\varepsilon_{\pm} = \frac{\varepsilon_{\sigma^+} + \varepsilon_{\sigma^-}}{2} \pm \sqrt{\left(\frac{\varepsilon_{\sigma^+} - \varepsilon_{\sigma^-}}{2}\right)^2 + |V^{\text{ex}}|^2}, \quad (9)$$

where $V^{\text{ex}} = V_{\downarrow\downarrow}^{\text{ex}} = V_{\uparrow\uparrow}^{\text{ex}*}$ and

$$\varepsilon_{\sigma^-} = \hbar\Omega_0 + \frac{1}{2}(V^{ee} + V^{hh} - 2V^{eh}) + V_{\uparrow\uparrow}^{\text{ex}}, \quad (10a)$$

$$\varepsilon_{\sigma^+} = \hbar\Omega_0 + \frac{1}{2}(V^{ee} + V^{hh} - 2V^{eh}) + V_{\downarrow\downarrow}^{\text{ex}}. \quad (10b)$$

Rewriting our model Hamiltonian within the space spanned by the electronic eigenstates $|\nu\rangle = |0\rangle, |\pm\rangle, |B\rangle$ yields

$$H = \sum_{\nu} \hbar\omega_{\nu} |\nu\rangle\langle\nu| + \sum_{\xi} \hbar\omega_{\xi} b_{\xi}^{\dagger} b_{\xi} + \sum_{\xi\nu} \hbar(g_{\xi}^e b_{\xi} + g_{\xi}^{h*} b_{\xi}^{\dagger}) |\nu\rangle\langle\nu| - \sum_{\nu\nu'} \hbar\bar{M}_{\nu\nu'} |\nu\rangle\langle\nu'| \quad (11)$$

with $\hbar\omega_{\nu} = \varepsilon_{\nu}$ and

$$g_{\xi}^e = (g_{\xi}^e - g_{\xi}^h) n_{\nu}, \quad (12)$$

where n_{ν} is the number of electron hole pairs present in the state $|\nu\rangle$, i.e., $n_0 = 0, n_{\pm} = 1, n_B = 2$. Finally, the dipole coupling in the eigenbasis $|\nu\rangle$ is described by the matrix \bar{M} with

$$\bar{M}_{\nu\nu'} = \sum_{ss'} S_{s\nu} M_{ss'} S_{s'\nu'}^*, \quad (13)$$

where $M_{ss'}$ represents the dipole coupling in the spin basis $|s\rangle$ and $S_{s\nu}$ provides the transformation between the two basis sets according to

$$|s\rangle = \sum_{\nu} S_{s\nu} |\nu\rangle. \quad (14)$$

The nonzero components of S are given explicitly by $S_{00} = S_{BB} = 1$, $S_{\sigma^{\pm}\pm} = |V^{\text{ex}}| / \sqrt{|V^{\text{ex}}|^2 + (\varepsilon_{\pm} - \varepsilon_{\sigma^{\pm}})^2}$, and $S_{\sigma^{\pm}\pm} = (\varepsilon_{\pm} - \varepsilon_{\sigma^{\pm}}) S_{\sigma^{\pm}\pm} / V^{\text{ex}*}$. Explicit expressions for the components of M follow from Eqs. (7) and (6)

$$M = \begin{pmatrix} 0 & \Omega_{\sigma^+}^* & \Omega_{\sigma^-} & 0 \\ \Omega_{\sigma^+} & 0 & 0 & \Omega_{\sigma^-}^* \\ \Omega_{\sigma^-} & 0 & 0 & \Omega_{\sigma^+}^* \\ 0 & \Omega_{\sigma^-} & \Omega_{\sigma^+} & 0 \end{pmatrix}, \quad (15)$$

where $\Omega_{\sigma^{\pm}} \equiv M_0 E_{\sigma^{\pm}} / \hbar$ is the Rabi frequency of the dipole transition to the $|\sigma^{\pm}\rangle$ single-pair state and $E_{\sigma^{\pm}}$ is the σ^{\pm} component of the laser field amplitude.

III. GENERAL SOLUTION FOR SEQUENCES OF ULTRAFAST PULSES

As in Ref. 62 we shall represent the dynamics of the system in terms of generating functions for phonon assisted density matrices. The following generating functions form a complete set of dynamical variables:

$$\rho_{\nu\nu'}(\{\alpha_{\xi}\},\{\beta_{\xi}\},t)=\langle\hat{\rho}_{\nu\nu'}(\{\alpha_{\xi}\},\{\beta_{\xi}\})\rangle. \quad (16)$$

The angle brackets denote the quantum-mechanical expectation value of the operators $\hat{\rho}_{\nu\nu'}$ defined as

$$\hat{\rho}_{\nu\nu'}(\{\alpha_{\xi}\},\{\beta_{\xi}\})=|\nu\rangle\langle\nu'|\exp\left(\sum_{\xi}\alpha_{\xi}b_{\xi}^{\dagger}\right)\exp\left(\sum_{\xi}\beta_{\xi}b_{\xi}\right). \quad (17)$$

α_{ξ} , β_{ξ} are auxiliary complex valued numbers. The time dependence of the expectation values $\rho_{\nu\nu'}$ reflects in the Heisenberg picture the time dependence of the operators $\hat{\rho}_{\nu\nu'}$. All components of the reduced electronic density matrix can be obtained by evaluating the generating functions in Eq. (16) at $\alpha_{\xi}=\beta_{\xi}=0$ while all phonon-assisted electronic density matrices are given by suitable derivatives of $\rho_{\nu\nu'}(\{\alpha_{\xi}\},\{\beta_{\xi}\},t)$ with respect to α_{ξ} and β_{ξ} taken again at $\alpha_{\xi}=\beta_{\xi}=0$.

To explore dynamical properties of the phonon system it is convenient to introduce the function

$$\begin{aligned} F(\{\alpha_{\xi}\},\{\beta_{\xi}\}) &\equiv \left\langle \exp\left(\sum_{\xi}\alpha_{\xi}b_{\xi}^{\dagger}\right)\exp\left(\sum_{\xi}\beta_{\xi}b_{\xi}\right) \right\rangle \\ &= \sum_{\nu} \rho_{\nu\nu}(\{\alpha_{\xi}\},\{\beta_{\xi}\}), \end{aligned} \quad (18)$$

where the second line follows by noting that within the space spanned by the states $|\nu\rangle$ the operator $\sum_{\nu}|\nu\rangle\langle\nu|$ acts as the identity. Using the Heisenberg equations for the operators $\hat{\rho}_{\nu\nu'}(\{\alpha_{\xi}\},\{\beta_{\xi}\})$ and then taking expectation values of the result yields exact closed form evolution equations for the phonon assisted generating functions which read

$$\begin{aligned} i\frac{\partial}{\partial t}\rho_{\nu\nu'}(\{\alpha_{\xi}\},\{\beta_{\xi}\}) &= -\hat{\Lambda}_{\nu\nu'}(\{\alpha_{\xi}\},\{\beta_{\xi}\})\rho_{\nu\nu'}(\{\alpha_{\xi}\},\{\beta_{\xi}\}) \\ &+ \sum_{\bar{\nu}}[\bar{M}_{\nu\bar{\nu}}^*\rho_{\bar{\nu}\nu'}(\{\alpha_{\xi}\},\{\beta_{\xi}\}) \\ &- \rho_{\nu\bar{\nu}}(\{\alpha_{\xi}\},\{\beta_{\xi}\})\bar{M}_{\bar{\nu}\nu'}^*], \end{aligned} \quad (19)$$

where the operator $\hat{\Lambda}_{\nu\nu'}(\{\alpha_{\xi}\},\{\beta_{\xi}\})$ is defined as

$$\begin{aligned} \hat{\Lambda}_{\nu\nu'}(\{\alpha_{\xi}\},\{\beta_{\xi}\}) &\equiv \sum_{\xi}[\hat{L}(\omega_{\xi},g_{\xi}^{\nu*}-g_{\xi}^{\nu'*},g_{\xi}^{\nu},\alpha_{\xi}) \\ &- \hat{L}(\omega_{\xi},g_{\xi}^{\nu'}-g_{\xi}^{\nu},g_{\xi}^{\nu'*},\beta_{\xi})] + \omega_{\nu} - \omega_{\nu'} \end{aligned} \quad (20)$$

with

$$\hat{L}(\omega,\kappa,\lambda,x)\equiv\omega x\partial_x+\kappa\partial_x+\lambda x. \quad (21)$$

The equations of motion (19) have to be complemented by initial conditions. Demanding, e.g., that at a time t_0 before the arrival of the pulses the dot is in the electronic ground state while the phonons are in thermal equilibrium imposes

$$\rho_{\nu\nu'}(t=t_0)=\delta_{\nu,0}\delta_{\nu',0}F_0(\{\alpha_{\xi}\},\{\beta_{\xi}\}), \quad (22)$$

where F_0 is the phononic generating function F [see Eq. (18)] evaluated for thermal phonons

$$F_0(\{\alpha_{\xi}\},\{\beta_{\xi}\})=\exp\left(\sum_{\xi}\alpha_{\xi}\beta_{\xi}N_{\xi}\right), \quad (23)$$

where $N_{\xi}=[\exp(\hbar\omega_{\xi}/K_B T)-1]^{-1}$ denotes the Bose distribution of the phonons at temperature T .

In the following the system is assumed to be excited by a sequence of ultrafast pulses with Rabi frequencies

$$\Omega_{\sigma}(t)=\sum_j\frac{f_{j\sigma}}{2}e^{i\varphi_{j\sigma}}\delta(t-t_j), \quad (24)$$

where σ can stand for σ^+ or σ^- and $f_{j\sigma}$ is the pulse area of the σ component of the j th pulse while $\varphi_{j\sigma}$ is the corresponding phase. A complete derivation of the solution to Eq. (19) valid for this ultrafast pulse limit will be given in Appendix A. In the time interval between the j th pulse and the arrival of the $(j+1)$ -th pulse we obtain

$$\rho_{\nu\nu'}(t)=e^{i\hat{\Lambda}_{\nu\nu'}(t-t_j)}[e^{-iQ^{(j)}}\rho^{(j)}e^{iQ^{(j)}}]_{\nu\nu'}, \quad (25)$$

where $\rho^{(j)}$ is the value of ρ at time $t=t_j$ immediately before the arrival of the j th pulse. $\exp(\pm iQ^{(j)})$ is a 4×4 matrix defined in Eq. (A14) that is independent of α_{ξ} and β_{ξ} and comprises the dependences on the parameters of the j th pulse. Thus, the product in brackets $[\dots]$ in Eq. (25) is a matrix product between 4×4 matrices. Then, for each combination ν,ν' we have to act with the operator $\exp[i\hat{\Lambda}_{\nu\nu'}(t-t_j)]$ on the α_{ξ} and β_{ξ} dependences which emerge from $\rho^{(j)}$. The action of this exponential operator on an arbitrary function of α_{ξ} and β_{ξ} is given explicitly by Eq. (A2) which is derived in Appendix B.

Finally, by using Eq. (25) we find a recurrence relation connecting the values of $\rho^{(j)}$ for subsequent pulses

$$\rho_{\nu\nu'}^{(j+1)}=e^{i\hat{\Lambda}_{\nu\nu'}(t_{j+1}-t_j)}[e^{-iQ^{(j)}}\rho^{(j)}e^{iQ^{(j)}}]_{\nu\nu'}. \quad (26)$$

Equations (25) and (26) together with the initial condition Eq. (22) provide a complete solution of Eq. (19) for an arbitrary sequence of ultrafast pulses of the form Eq. (24).

Our solution is exact for a QD in the strong confinement limit. However, it is worth noting that the Hamiltonian (11) can still be used even when it is no longer justified to treat excitons and biexcitons as product states representing uncorrelated electron hole pairs as is implied by the strong confinement. Then, correlated pair states can be constructed, e.g., from configuration interaction^{6,38,41,56} or tight binding⁴² calculations with extended basis sets which can be used as basis states in Eq. (11). Most of the steps in our derivation are not affected by this reinterpretation of the model. There are only three differences: (i) the electronic energies are no longer given by Eqs. (8) and (9), (ii) the carrier-phonon coupling has to be calculated by using the correlated wave functions, and (iii) the dipole matrix elements have to be determined for the correlated states.

The modification of energies according to (i) amounts merely in an exchange of parameters. This is also formally true for the changes of the carrier-phonon coupling. In fact, our formal derivation does not require any specific form of the couplings g_{ξ}^{ν} and thus our general results can be used with couplings g_{ξ}^{ν} that are evaluated for correlated states. It

should be noted, however, that for correlated states the factorization in Eq. (12) does not hold in general. Recent measurements indicate³⁰ strong deviations from Eq. (12) when the system is far from the strong confinement limit, as applies to the interface QDs studied in Ref. 30. Below, we will discuss a few consequences of this factorization that can be used to monitor the validity of the strong confinement assumption.

Also for any modification of \bar{M} it is still possible to construct the exact solution. Indeed, the solution is affected by such changes via a different form of the matrix $\exp(\pm iQ^{(j)})$ in Eq. (A14). It is clear, however, from the derivation that even in the most general case $\exp(\pm iQ^{(j)})$ can be constructed by a diagonalization of a 4×4 matrix. We note, however, that experimental evidence⁴⁶ suggests that the relations between the dipole matrix elements as expressed by Eq. (15) are typically fulfilled even for interface dots which are usually not in the strong confinement limit. It is thus likely that $\exp(\pm iQ^{(j)})$ is reasonably represented by Eq. (A14) for correlated states, too.

IV. SINGLE PULSE SOLUTION

We shall now apply our general scheme to the simplest special case: the excitation by a single ultrafast pulse. We assume that the pulse reaches the dot at time $t_1=0$ such that the corresponding Rabi frequencies read

$$\Omega_{\sigma}(t) = \frac{f_{\sigma}}{2} e^{i\varphi_{\sigma}} \delta(t), \quad (27)$$

where σ stands for σ^+ or σ^- . We shall concentrate on a situation where transitions from the electronic ground state $|0\rangle$ to the excitonic eigenstates $|\pm\rangle$ couple selectively to orthogonally linear polarized light; a behavior which has been observed in many experiments.^{10,16,32,77} Within our model we achieve this situation by setting $V_{\uparrow\uparrow}^{\text{ex}} = V_{\downarrow\downarrow}^{\text{ex}}$ and $V^{\text{ex}} = |V^{\text{ex}}\rangle$ [see Eqs. (8)–(10)] whereby the transformation matrix S simplifies to

$$S = \begin{pmatrix} 1 & 0 & 0 & 0 \\ 0 & \frac{1}{\sqrt{2}} & \frac{1}{\sqrt{2}} & 0 \\ 0 & \frac{1}{\sqrt{2}} & -\frac{1}{\sqrt{2}} & 0 \\ 0 & 0 & 0 & 1 \end{pmatrix}. \quad (28)$$

In the following subsections we shall illustrate pertinent features of our solution by working out explicit results for this specific case.

A. Diagonal generating functions and electronic occupations

By using the solution Eq. (25) together with the initial conditions Eq. (22) and the specific assumptions Eqs. (27) and (28) we obtain for the diagonal elements (i.e., $\nu=\nu'$) of the generating functions explicitly

$$\begin{aligned} \rho_{\nu\nu}(\{\alpha_{\xi}\}, \{\beta_{\xi}\}, t) &= F_0(\{\alpha_{\xi}\}, \{\beta_{\xi}\}) \left\{ \theta(-t) \delta_{\nu,0} + \theta(t) C_{\nu} \right. \\ &\quad \left. \times \exp\left(\sum_{\xi} [\gamma_{\xi}^{\nu} (e^{i\omega_{\xi} t} - 1) \alpha_{\xi} + \gamma_{\xi}^{\nu*} (e^{-i\omega_{\xi} t} - 1) \beta_{\xi}] \right) \right\}, \end{aligned} \quad (29)$$

where $\gamma_{\xi}^{\nu} \equiv g_{\xi}^{\nu} / \omega_{\xi}$ are dimensionless coupling constants. F_0 is the phononic generating function in equilibrium defined in Eq. (23) and $\theta(t)$ is the unit step function. Finally, C_{ν} are the electronic occupations after the pulse, i.e., $C_{\nu} \equiv \rho_{\nu\nu}(\alpha_{\xi}=\beta_{\xi}=0)$ for $t>0$, which evaluate to

$$C_0 = \frac{1}{4} [\cos(f_+) + \cos(f_-)]^2, \quad (30a)$$

$$C_{\pm} = \frac{1}{4} |W_{\pm}|^2, \quad (30b)$$

$$C_B = \frac{1}{4} [\cos(f_+) - \cos(f_-)]^2, \quad (30c)$$

with

$$W_{\pm} \equiv \frac{i}{\sqrt{2}} [(e^{i\varphi_{\sigma^+}} \pm e^{i\varphi_{\sigma^-}}) \sin(f_+) + (e^{i\varphi_{\sigma^+}} \mp e^{i\varphi_{\sigma^-}}) \sin(f_-)], \quad (31)$$

and

$$f_{\pm} \equiv \frac{f_{\sigma^+} \pm f_{\sigma^-}}{2}. \quad (32)$$

The occupations of the electronic eigenstates C_{ν} are constants, independent of time and phonon degrees of freedom. This is expected for a single pulse excitation, because before the arrival of the pulse there is no phonon induced dynamics and afterwards the C_{ν} cannot be changed by pure dephasing interactions alone. In contrast, for a multipulse setup phonons may have a profound impact on electronic occupations as seen, e.g., in the two-pulse control of the electron density in a QD which reflects the loss of coherence due to pure dephasing.⁶²

We shall briefly mention some characteristic polarization dependences of the occupations C_{ν} . For excitation by circular polarized light, e.g., σ^+ , we find by setting $f_{\sigma^+}=f$, $f_{\sigma^-}=0$ in Eqs. (31) and (32) that $f_{\pm}=f/2$ and $W_{\pm} = i\sqrt{2} e^{i\varphi_{\sigma^+}} \sin(f/2)$ which yields [see Eqs. (30)]

$$C_0 = \cos^2(f/2), \quad C_{\pm} = \frac{1}{2} \sin^2(f/2), \quad C_B = 0. \quad (33)$$

The excitonic occupation is equally divided between the states $|\pm\rangle$ while the occupation of the biexciton state vanishes reflecting the well known selection rules for the excitation of biexcitons, which have recently been confirmed experimentally also for QDs.⁶⁴ As illustrated in Fig. 1(a), the total excitonic occupation $C_X \equiv C_+ + C_-$ rises monotonously from zero at $f=0$ to its maximum at $f=\pi$, where all the

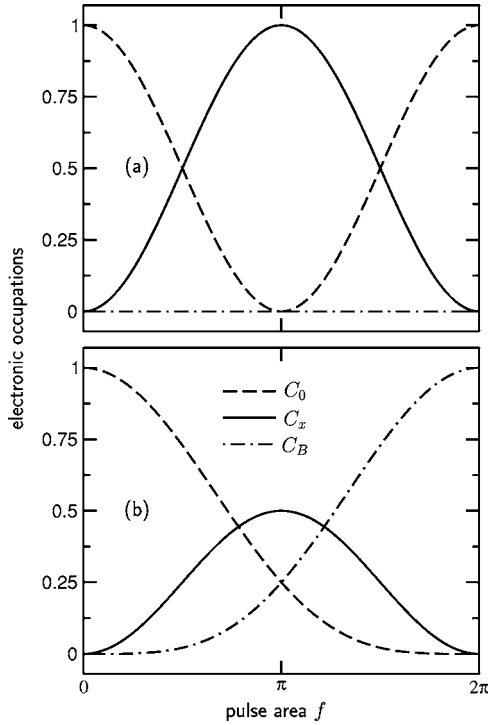


FIG. 1. Occupations of the ground [C_0] and the biexciton state [C_B] as well as the total excitonic occupation [$C_x=C_++C_-$]: (a) after ultrafast σ^+ excitation with $f_{\sigma^+}=f$, $f_{\sigma^-}=0$; (b) after ultrafast excitation with a linearly polarized pulse with $f_{\sigma^+}=f_{\sigma^-}=f/2$, $\varphi_{\sigma^+}=\varphi_{\sigma^-}=\varphi$.

excitation is in single exciton states, i.e., $C_x(f=\pi)=1$. Correspondingly, the ground state occupation C_0 falls from one to zero. This behavior closely resembles the π rotation on the Bloch sphere of a two-level system without phonon coupling. It should be noted, however, that due to the presence of the phonon coupling the radius of the Bloch sphere is not conserved in our model. A further difference to the two level case is that the total excitonic excitation is now equally divided over the two electronic eigenstates $|\pm\rangle$. The system is thus in a superposition state and not in a stationary electronic state when $C_x(f=\pi)=1$ is reached.

A very different scenario is obtained when linearly polarized light is used, which can be modeled by setting $f_{\sigma^+}=f_{\sigma^-}=f/2$ resulting in $f_+=f/2$ and $f_-=0$ and thus $W_{\pm}=(i/\sqrt{2})(e^{i\varphi_{\sigma^+}}\pm e^{i\varphi_{\sigma^-}})\sin(f/2)$. Obviously, one of the factors W_{\pm} vanishes when the condition $\varphi_{\sigma^+}=\varphi_{\sigma^-}+n\pi$ holds which corresponds to either x or y polarized light. Let us discuss the case $\varphi_{\sigma^+}=\varphi_{\sigma^-}=\varphi$, where W_- vanishes and $|+\rangle$ is the only occupied exciton state. To simplify the notation, from now on we shall refer to this particular choice when speaking of linear excitation conditions. Equations (30) yield in this case

$$C_0 = \cos^4(f/4), \quad C_+ = \frac{1}{2} \sin^2(f/2),$$

$$C_- = 0, \quad C_B = \sin^4(f/4). \quad (34)$$

Here, the total excitonic density is given by $C_x=C_+$ and reaches its maximum at $f=\pi$ as for the σ^+ excitation. How-

ever, at $f=\pi$ we have only $C_x=1/2$ because now the ground and the biexciton state are not empty. C_0 , C_x and C_B are plotted in Fig. 1(b) vs f for linear excitation conditions. Interestingly, at $f=2\pi$ the system is not back in the ground state even though there is no occupation of single exciton states. Instead, all the excitation is in the biexciton state. To return the system to the ground state a 4π -pulse is required. Indeed, recent measurements of Rabi rotations in QDs (Refs. 72 and 78) have given experimental evidence that the Rabi period increases when in addition to excitons also biexcitons are involved. Thus, biexcitons strongly affect excitonic occupations. In particular it is impossible to prepare a purely excitonic state with a single linearly polarized ultrafast pulse; the only electronic eigenstates that could be prepared in this way are $|0\rangle$ and $|B\rangle$.

B. Coherent phonon generation

We shall now discuss the coherent phonon amplitudes $\langle b_{\xi} \rangle$ which can be used to calculate finite lattice distortions and related lattice polarizations⁷⁹ as well as the corresponding relative volume changes.⁸⁰ The impact of these lattice deformations is directly observable, e.g., in ultrafast deflection experiments.⁸¹ Using Eq. (18) together with Eq. (29) yields

$$\langle b_{\xi} \rangle = \partial_{\beta_{\xi}} F|_{\alpha_{\xi}=\beta_{\xi}=0} = \theta(t)(e^{-i\omega_{\xi}t} - 1) \sum_{\nu} \gamma_{\xi}^{\nu*} C_{\nu}. \quad (35)$$

In the strong confinement limit Eq. (12) can be used resulting in a factorization in Eq. (35) according to

$$\langle b_{\xi} \rangle = a_{\xi}(t)A(f) \quad (36)$$

with

$$a_{\xi}(t) \equiv \theta(t) \frac{g_{\xi}^{e*} - g_{\xi}^{h*}}{\omega_{\xi}} (e^{-i\omega_{\xi}t} - 1), \quad (37)$$

$$A(f) \equiv \sum_{\nu} n_{\nu} C_{\nu}. \quad (38)$$

It should be noted that in the general case where γ_{ξ}^{\pm} is not proportional to γ_{ξ}^B , Eq. (35) predicts that the ξ dependence of $\langle b_{\xi} \rangle$ changes as a function of f when both excitonic and biexcitonic occupations are created, because then the relative weights of γ_{ξ}^{\pm} and γ_{ξ}^B vary with the excitation density. In contrast, in the strong confinement limit a f variation yields only a scaling of $\langle b_{\xi} \rangle$ with the prefactor $A(f)$ which is the same for all ξ . For σ^+ excitation we obtain $A(f)=C_x=\sin^2(f/2)$ which coincides with the result found for the electronic two-level system with pure phonon dephasing coupling.⁸⁰ For linear excitation conditions we find $A(f)=C_++C_B=\sin^2(f/2)/2+2\sin^4(f/4)$. Both cases are illustrated in Fig. 2. It turns out that for pulse areas $f<\pi$ the phonon amplitude for circular polarization is larger than in the linear case. It peaks at $f=\pi$ when all the excitation is in excitonic states [see Fig. 1(a)]. In contrast, after linear excitation the coherent phonon amplitude $A(f)$ still rises when f is increased from π to 2π . In this interval more coherent phonons are produced with linearly than with circularly po-

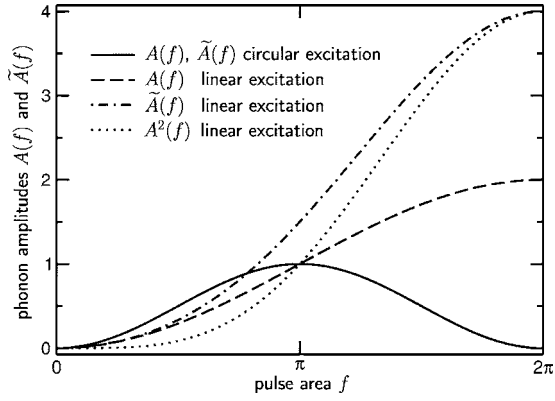


FIG. 2. Coherent phonon amplitude $A(f)$ [see Eq. (38)] after excitation with an ultrafast pulse: circularly polarized excitation (solid line); linearly polarized excitation (dashed line); amplitude $\tilde{A}(f)$ of the optically generated N^{opt} phonon occupation [see Eq. (42)] after linearly polarized excitation (dash-dotted line); amplitude $A^2(f)$ of the coherent phonon density N^{coh} after linearly polarized excitation (dotted line).

larized light. For linear excitation the maximal phonon amplitude is reached at $f=2\pi$ where only the biexciton state is occupied [see Fig. 1(b)]. The maximum of $A(f)$ is twice as large for the linear than for the circular polarization, reflecting the fact that in the former case the lattice is deformed by the presence of two electron-hole pairs instead of one in the latter case.

C. Nonequilibrium phonon occupations and coherences

In a nonequilibrium situation the generation of coherent phonon amplitudes is not the only modification of the lattice properties. Instead, also the occupations $\langle b_{\xi}^{\dagger} b_{\xi} \rangle$ of phonon number states will change and in addition coherences $\langle b_{\xi}^{\dagger} b_{\xi'} \rangle$ between different phonon modes $\xi \neq \xi'$ will occur. The components

$$N_{\xi\xi'} \equiv \langle b_{\xi}^{\dagger} b_{\xi'} \rangle \quad (39)$$

of the phononic density matrix account for both effects. For bulk phonons where the index ξ comprises a momentum \mathbf{q} , the quantity $N_{\xi\xi'}$ can be used to construct a corresponding Wigner function in order to get a real space picture of the phonon distribution.^{62,82} In general, $N_{\xi\xi'}$ together with the phonon dispersion ω_{ξ} comprises the information on the spatial energy distribution. Changes of the latter are responsible for the phonon contribution to heat transport which is measurable in bolometric experiments.^{83,84} From Eqs. (18) and (29) we get

$$\begin{aligned} N_{\xi\xi'} &= \partial_{\alpha_{\xi}} \partial_{\beta_{\xi'}} F \Big|_{\alpha_{\xi}=\beta_{\xi}=0} \\ &= \delta_{\xi\xi'} N_{\xi} + \theta(t) (e^{i\omega_{\xi}t} - 1) (e^{-i\omega_{\xi'}t} - 1) \sum_{\nu} \gamma_{\xi'}^{*\nu} \gamma_{\xi}^{\nu} C_{\nu}, \end{aligned} \quad (40)$$

which in the strong confinement limit reduces to

$$N_{\xi\xi'} = \delta_{\xi\xi'} N_{\xi} + a_{\xi}^{*}(t) a_{\xi'}(t) \tilde{A}(f) \quad (41)$$

with

$$\tilde{A}(f) \equiv \sum_{\nu} n_{\nu}^2 C_{\nu}, \quad (42)$$

where $a_{\xi}(t)$ has been defined in Eq. (37).

The first term in Eq. (41) is the spatially homogeneous equilibrium density of phonons while the second marks the optically generated nonequilibrium contribution $N_{\xi\xi'}^{\text{opt}} \equiv N_{\xi\xi'} - \delta_{\xi\xi'} N_{\xi}$. Interestingly, $N_{\xi\xi'}^{\text{opt}}$ exhibits the same time dependence as the coherent phonon density that is conventionally defined by $N_{\xi\xi'}^{\text{coh}} \equiv \langle b_{\xi} \rangle^* \langle b_{\xi'} \rangle$. However, still N^{coh} does not coincide with N^{opt} , because the pulse area dependent amplitudes are different, i.e., $\tilde{A}(f) \neq A^2(f)$ (see Fig. 2). In particular, for low pulse areas we find $N^{\text{opt}} \propto f^2$ while $N^{\text{coh}} \propto f^4$. The difference between N^{opt} and N^{coh} demonstrates that the optically generated nonequilibrium phonons are in general not in a coherent state even in the strong confinement limit where N^{opt} and N^{coh} have identical time dependences. An exception is the pulse area $f=2\pi$ where all the excitation is in the biexciton state. Here, $A^2(f) = \tilde{A}(f)$ and thus we find $N^{\text{coh}} = N^{\text{opt}}$ which indicates that in this case the nonequilibrium phonon density is fully coherent.

D. Electronic coherences

We shall now discuss the behavior of the off-diagonal elements of the electronic density matrix which are commonly referred to as electronic coherences. We obtain

$$\begin{aligned} C_{\nu\nu'} &\equiv \rho_{\nu\nu'}(\{\alpha_{\xi}\}, \{\beta_{\xi'}\}, t) \Big|_{\alpha_{\xi}=\beta_{\xi}=0} \\ &= \theta(-t) \delta_{\nu,0} \delta_{\nu',0} + \theta(t) \bar{C}_{\nu\nu'} \exp[i t (\bar{\omega}_{\nu} - \bar{\omega}_{\nu'})] \\ &\quad \times \exp\left(-\sum_{\xi} N_{\xi} (\gamma_{\xi}^{\nu} - \gamma_{\xi}^{\nu'}) (e^{-i\omega_{\xi}t} - 1)\right) \\ &\quad \times \exp\left(\sum_{\xi} \gamma_{\xi}^{\nu'*} (\gamma_{\xi}^{\nu} - \gamma_{\xi}^{\nu'}) (e^{-i\omega_{\xi}t} - 1)\right) \\ &\quad \times \exp\left(\sum_{\xi} \gamma_{\xi}^{\nu} (\gamma_{\xi}^{\nu'*} - \gamma_{\xi}^{\nu'}) (e^{i\omega_{\xi}t} - 1)\right), \end{aligned} \quad (43)$$

where $\bar{\omega}_{\nu} \equiv \omega_{\nu} - \sum_{\xi} \omega_{\xi} |\gamma_{\xi}^{\nu}|^2$ are polaron shifted electronic frequencies. The coefficients $\bar{C}_{\nu\nu'} = \bar{C}_{\nu\nu'}^{*}$ depend only on $f_{\sigma^{\pm}}$ and $\varphi_{\sigma^{\pm}}$. For the diagonal elements we have $\bar{C}_{\nu\nu} = C_{\nu}$, where the C_{ν} are known from Eq. (30). The off-diagonal elements will be given below.

We shall distinguish coherences between states with the same number of electron hole pairs (intraband coherences) from coherences between states with different numbers of electron hole pairs (interband coherences). First, we will focus on intraband coherences and then come back to interband coherences later.

1. Exciton-exciton coherences and spin densities

There is only one intraband coherence in our model, namely, C_{+-} . It plays a decisive role for spin densities as is

most clearly seen by looking at the operator $c_{\uparrow}^{\dagger}c_{\uparrow}$ which counts the number of spin up electrons in the conduction band. Within our restricted basis set $c_{\uparrow}^{\dagger}c_{\uparrow}$ can be replaced by the projector $|\sigma^{-}\rangle\langle\sigma^{-}|+|B\rangle\langle B|$. Together with Eqs. (14) and (28) we thus obtain

$$\langle c_{\uparrow}^{\dagger}c_{\uparrow} \rangle = \frac{1}{2}(C_{+} + C_{-} - 2 \operatorname{Re}[C_{+-}]) + C_B, \quad (44)$$

and analogously for the density of spin down electrons

$$\langle c_{\downarrow}^{\dagger}c_{\downarrow} \rangle = \frac{1}{2}(C_{+} + C_{-} + 2 \operatorname{Re}[C_{+-}]) + C_B, \quad (45)$$

where C_{+-} is found from Eq. (43)

$$C_{+-}(t) = \theta(t)\bar{C}_{+-} \exp[it(\bar{\omega}_{+} - \bar{\omega}_{-})] \quad (46)$$

with

$$\bar{C}_{+-} = \frac{W_{+}^{*}W_{-}}{4}. \quad (47)$$

For selective excitations of the eigenstates $|\pm\rangle$ by linear polarized light either W_{+} or W_{-} is zero, \bar{C}_{+-} vanishes and thus the spin densities $\langle c_{\uparrow}^{\dagger}c_{\uparrow} \rangle$ and $\langle c_{\downarrow}^{\dagger}c_{\downarrow} \rangle$ are independent of time in this case and equal the sum $C_x/2 + C_B$. In contrast, σ^{+} excitation leads to the well known spin oscillations which reflect the energetic splitting between $|+\rangle$ and $|-\rangle$ due to the exchange interaction

$$\langle c_{\uparrow}^{\dagger}c_{\uparrow} \rangle = \frac{1}{2} \sin^2(f/2) \{1 - \cos[(\bar{\omega}_{+} - \bar{\omega}_{-})t]\}. \quad (48)$$

It is worth emphasizing that these oscillations are undamped only in the strong confinement limit; any finite difference between γ_{ξ}^{+} and γ_{ξ}^{-} will lead according to Eq. (43) to a phonon induced pure dephasing of the intraband coherence \bar{C}_{+-} , which will be also reflected in the spin densities.

2. Interband coherences and optical polarization

Calculating the expectation value of the optical polarization operator Eq. (7) within the basis $|\nu\rangle$ yields

$$\begin{aligned} \langle \hat{\mathbf{P}} \rangle = & \frac{M_0^{*}}{\sqrt{2}} \{ (\mathbf{e}_{\sigma^{+}} + \mathbf{e}_{\sigma^{-}})C_{0+} + (\mathbf{e}_{\sigma^{+}} - \mathbf{e}_{\sigma^{-}})C_{0-} + (\mathbf{e}_{\sigma^{-}} + \mathbf{e}_{\sigma^{+}})C_{+B} \\ & + (\mathbf{e}_{\sigma^{-}} - \mathbf{e}_{\sigma^{+}})C_{-B} \}, \end{aligned} \quad (49)$$

where Eq. (28) has been used for the transformation matrix $S_{\sigma\nu}$. Thus, the optical properties of our system are fully determined by $C_{0\pm}$ and $C_{\pm B}$. Assuming again strong confinement conditions we can use Eq. (12) together with Eq. (43) and obtain

$$C_{0\pm} = \theta(t)\bar{C}_{0\pm} e^{-i\bar{\omega}_{\pm}t} G_{\text{GET}}(t), \quad (50)$$

$$C_{\pm B} = \theta(t)\bar{C}_{\pm B} e^{-i(\bar{\omega}_B - \bar{\omega}_{\pm})t} G_{\text{EBT}}(t), \quad (51)$$

where the coefficients $\bar{C}_{\nu\nu'}$ are given by

$$\bar{C}_{0\pm} = [\cos(f_{+}) + \cos(f_{-})] \frac{W_{\pm}}{4}, \quad (52)$$

$$\bar{C}_{\pm B} = [\cos(f_{+}) - \cos(f_{-})] \frac{W_{\pm}^{*}}{4} e^{i(\varphi_{\sigma^{+}} + \varphi_{\sigma^{-}})}. \quad (53)$$

The temporal envelope functions G_{GET} and G_{EBT} for the ground state-exciton transition (GET) and the exciton-biexciton transition (EBT) are given by

$$G_{\text{GET}}(t) = g(t)s(t), \quad (54)$$

$$G_{\text{EBT}}(t) = g(t)s^3(t), \quad (55)$$

with

$$g(t) = \exp \left[- \sum_{\xi} |\gamma_{\xi}|^2 [1 - \cos(\omega_{\xi}t)] (1 + 2N_{\xi}) \right], \quad (56)$$

$$s(t) = \exp \left[- i \sum_{\xi} |\gamma_{\xi}|^2 \sin(\omega_{\xi}t) \right]. \quad (57)$$

The factors $e^{-i\bar{\omega}_{\pm}t}$ and $e^{-i(\bar{\omega}_B - \bar{\omega}_{\pm})t}$ in Eqs. (50) and (51) describe electronic oscillations of the coherences $C_{0\pm}$, $C_{\pm B}$ with polaron shifted transition frequencies. The four transition frequencies are all different provided that the exchange interaction V^{ex} does not vanish. In the spectral regime they correspond to four separate zero phonon lines (ZPL). An examination of the density dependent prefactors $\bar{C}_{\nu\nu'}$ confirms again the well known selection rules. For circular polarizations $C_{\pm B}$ vanishes while $C_{0+} = C_{0-} \neq 0$ in this case resulting in two ZPL's in the spectrum, split by the exchange interaction. In contrast, for excitations of the eigenstates $|\pm\rangle$ by linear polarized light one of the pairs of transition amplitudes C_{0+} and C_{+B} or C_{0-} and C_{-B} vanishes. Again, we see only two ZPLs which now correspond to one GET and one EBT. In order to see simultaneously four separate ZPLs a general excitation is required which is neither circular nor a linear polarization that selectively couples to one of the excitonic eigenstates.

The nonvanishing coefficients for σ^{+} excitation are

$$\bar{C}_{0\pm} = ie^{i\varphi_{\sigma^{+}}} \tilde{C}_{0\pm}, \quad \tilde{C}_{0\pm} = \frac{\sqrt{2}}{4} \sin(f),$$

while for linear excitation conditions we have

$$\bar{C}_{0+} = ie^{i\varphi} \tilde{C}_{0+}, \quad \tilde{C}_{0+} = \frac{\sqrt{2}}{4} [\cos(f/2) + 1] \sin(f/2),$$

$$\bar{C}_{+B} = ie^{i\varphi} \tilde{C}_{+B}, \quad \tilde{C}_{+B} = \frac{\sqrt{2}}{4} [1 - \cos(f/2)] \sin(f/2).$$

Apart from constant phase factors, the $\bar{C}_{\nu\nu'}$ are determined by the real factors $\tilde{C}_{\nu\nu'}$ which are plotted in Fig. 3 versus the pulse area f . For circular polarization C_{0+} vanishes at $f = 2n\pi$, $n=0,1,\dots$, when the system is in the electronic ground state, and at $f = (2n+1)\pi$, when the system is in a superposition of the $|\pm\rangle$ states. In contrast, for linear excitation conditions $C_{0+} \neq 0$ at $f = (2n+1)\pi$ because now the system is in a superposition of the states $|0\rangle$, $|+\rangle$ and $|B\rangle$ (see Fig. 1). Also from Fig. 1 the system is known to be in the electronic ground state at $f = 4n\pi$ and in the biexciton state at

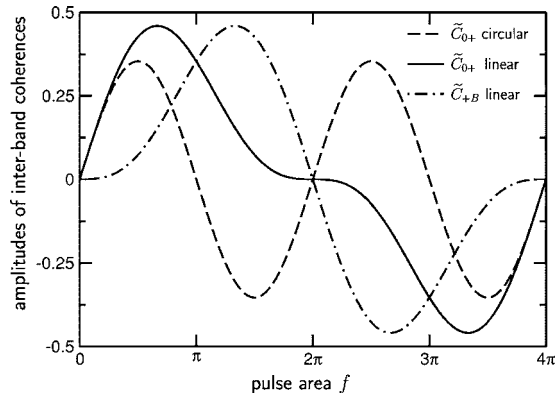


FIG. 3. Amplitudes of interband coherences \tilde{C}_{0+} after circular (dashed) and after linear (solid) excitation; \tilde{C}_{+B} after the same linear excitation (dot-dashed).

$f=(2n+1)2\pi$, $n=0,1,\dots$. For all other pulse areas a superposition of electronic states is created. The preparation of an electronic eigenstate ($|0\rangle$ or $|B\rangle$) at $f=n2\pi$ is reflected by vanishing coherences C_{0+} and C_{+B} at these pulse areas which also implies a vanishing optical polarization in these cases. Moreover, by expanding Eqs. (52) and (53) it is seen that $C_{0\pm} \propto f$ in the limit $f \rightarrow 0$ while $C_{\pm B} \propto f^3$ (if $C_{\pm B} \neq 0$). This difference explains why \tilde{C}_{+B} rises much slower than \tilde{C}_{0+} for low pulse areas (see Fig. 3). Equal finite amplitudes of these transitions are reached at the pulse areas $f=(2n+1)\pi$.

All four ZPL's acquire phonon sidebands due to the carrier-phonon interaction which are determined in the time domain by the factors $g(t)$ and $s(t)$ in Eqs. (54) and (55). The factor $g(t)$ is real and describes the decay of the polarization due to pure dephasing, while $s(t)$ is a phase factor. The function $G_{\text{GET}}(t)=g(t)s(t)$ is known from the time dependence of the linear response of the two-level model.⁶¹⁻⁶³ Its temporal and spectral properties have been discussed previously for various phonon coupling schemes and different models for the electronic confinement.^{12,61-63,85} It has been established that the acoustic phonon coupling via the deformation potential or the piezoelectric coupling provide the most efficient pure dephasing mechanisms.^{61,82,86} The resulting behavior of $g(t)$ is typically a rapid initial drop which eventually reaches a finite plateau. In the spectral domain the finite value of the plateau corresponds to an unbroadened ZPL which is superimposed on a broad background due to the initial decay. The broadening of the ZPL itself cannot be attributed to pure dephasing processes.

Interestingly, Eqs. (54) and (55) demonstrate that the amplitudes of all four transitions decay with the same temporal envelope defined by the factor $g(t)$. Within the strong confinement limit this is an exact result. It should be noted, however, that deviations from the relation $\gamma_{\xi}^{\nu} = \gamma_{\xi} n_{\nu}$ [see Eq. (12)] will, according to Eq. (43), result in different time dependences for each of the four amplitudes. In fact, the luminescence measurements of acoustic phonon sidebands in interface QDs, that were far from the strong confinement limit, show broader sidebands for the EBT than for the GET line implying in real time that EBTs decay faster than GETs.

Another interesting feature of our solution is that the phase of EBTs is determined by $s(t)^3$ [see Eq. (55)] instead

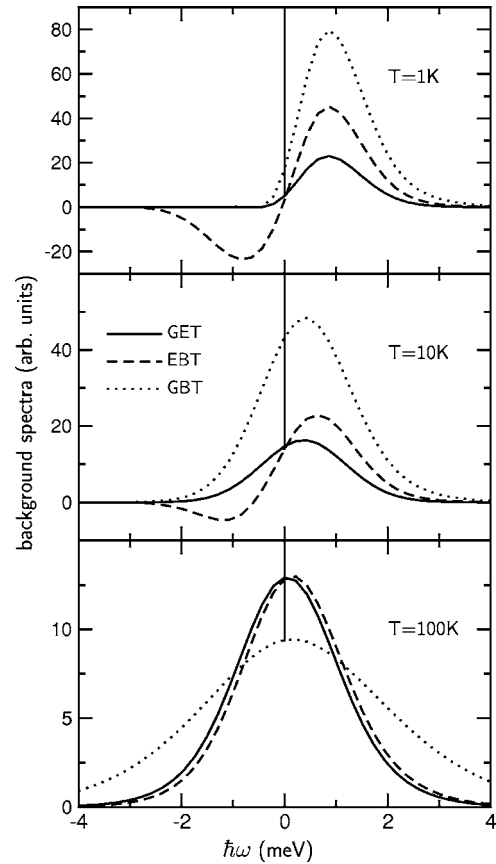


FIG. 4. Background spectra calculated at temperatures $T=1,10,100$ K for the ground state to exciton transition G_{GET} , the exciton to biexciton transition G_{EBT} and the ground state to biexciton transition G_{GBT} . The zero of energy $\hbar\omega=0$ is at the position of the respective ZPLs (vertical lines).

of $s(t)$ which applies to GETs. This implies that even though the absolute values of the time domain amplitudes evolve identically for both GETs and EBTs, the respective spectra have different shapes.

To illustrate these features we have calculated GET and EBT spectra. For simplicity only the contribution from the deformation potential coupling to bulk phonons⁶¹⁻⁶³ has been accounted for and a spherical harmonic oscillator model for the electronic confinement has been used.^{62,63} All material parameters were set for GaAs which may be regarded as a prototype for a material with weak carrier-phonon coupling.⁶¹ The spherical symmetry implies a vanishing exchange coupling which has, however, no effect on the functions $G_{\text{GET}}(t)$ and $G_{\text{EBT}}(t)$ that define the spectra. Previous calculations for the two-level case have shown only little sensitivity on the precise choice of the confinement model.^{12,61-64,85} For GaAs-like materials without external bias fields the deformation potential coupling has been found to dominate.⁶¹ The piezoelectric coupling may give a large quantitative contribution to the dephasing in strongly polar materials such as, e.g., GaN which, however, typically exhibits a qualitative behavior similar to the deformation potential contribution.⁸⁶ Shown in Fig. 4 are so-called background spectra for three temperatures T , i.e., we have subtracted the finite long time values from $G_{\text{GET}}(t)$ and

$G_{\text{EBT}}(t)$, normalized the results to their respective values at $t=0$ and then taken the Fourier transforms (see Ref. 62 also). Subtracting the asymptotic values removes the ZPLs from the spectra and allows us to concentrate on the broad background. Plotted in Fig. 4 is the real part of the resulting Fourier transforms which gives a frequency space representation of $G_{\text{GET}}(t)$ and $G_{\text{EBT}}(t)$. The positions of the ZPLs are indicated by vertical lines as a guide to the eye. The physical meaning of these real background spectra is most transparent for GETs at small f in which case they can be identified with the linear absorption spectra (apart from the ZPL which has been removed). For larger f and especially for G_{EBT} , which contributes only to the nonlinear response, the interpretation is more involved because there is no one to one correspondence between a spectral component in the emission and in the excitation due to the nonlinear character of the signal. A spectral feature at some frequency ω in the emission can thus not be directly interpreted as an absorption or gain at this frequency. It should be stressed that these calculations cannot be compared with the luminescence spectra reported in Ref. 30 not only because the latter were performed on weakly confined QDs but also because our calculation refers to a very different experimental situation, where a spectral decomposition of a coherent nonlinear emission is recorded after an ultrafast pulsed excitation.

As seen in Fig. 4 there is a significant difference between GET and EBT spectra especially at low temperatures. GET spectra have a positive sign for all ω while the sign of the EBT spectra depends on ω . At $T=0$ the GET spectrum vanishes below the corresponding ZPL, while the EBT spectrum is nonzero on both sides of the ZPL. With growing temperature both GET and EBT spectra become more symmetric and approach each other at large T . Recalling that the linear absorption is proportional to the GET spectra suggests a simple physical interpretation for the ω and T dependences of the latter: At $T=0$ K light can be absorbed only at frequencies above the ZPL, because at $T=0$ K no thermal phonons are present and the absorption reflects transitions from the electronic ground state with no phonons to single pair states with $n=0, 1, 2, \dots$, phonons corresponding to transition frequencies above the ZPL. Transitions assisted by phonon absorption processes become available at finite T due to the buildup of thermal phonon occupations yielding positive non-vanishing GET spectra below the ZPL. Note, that a positive value of the GET spectra indicates absorption while a negative value would correspond to gain. At large T where $N_\xi \gg 1$, phonon absorption and creation processes become equally probable resulting in absorption spectra symmetric around the ZPL. The nonlinear character of EBTs prohibits an equally simple interpretation of the corresponding spectra and further considerations are required to relate the nonlinear emission to absorption or gain.

It is instructive to trace back the above spectral features to our analytical time domain formulas (54) and (55). To this end we expand the latter in the limit $T \rightarrow 0$ up to leading order in γ_ξ , which is valid for not too large carrier-phonon couplings

$$G_{\text{GET}}(t) \approx \text{const} + \sum_{\xi} |\gamma_{\xi}|^2 e^{-i\omega_{\xi} t}, \quad (58)$$

$$G_{\text{EBT}}(t) \approx \text{const} + \sum_{\xi} |\gamma_{\xi}|^2 (2e^{-i\omega_{\xi} t} - e^{i\omega_{\xi} t}). \quad (59)$$

Obviously, G_{GET} oscillates only with positive frequencies while G_{EBT} comprises both positive and negative frequency components. This translates directly to the single sided GET spectra at $T=0$ and also explains the spectral components below the ZPL in the EBT case. Furthermore, the amplitude of the EBT spectrum above the respective ZPL should be twice as large as for the GET case, while below the ZPL the EBT spectrum should be the negative mirror image of the GET spectra above the ZPL. All of these relations derive directly from our analytical formulas and do not depend on specific details of the coupling γ_{ξ} or the phonon dispersion ω_{ξ} . They thus constitute generic features which are nicely illustrated by the numerical results in Fig. 4. At large T the exponents contained in G_{GET} and G_{EBT} are dominated by the terms with the Boltzmann factor N_{ξ} . Thus, the phase factors $s(t)$ and $s(t)^3$ become of minor importance and the spectra reflect asymptotically the Fourier transform of the real function g which is symmetric. This explains why at large T the GET and EBT spectra are both symmetric and have identical shapes as is seen in Fig. 4.

It should be noted that the phases of the corresponding nonlinear polarizations are determined—apart from a constant common phase—by the real coefficients \tilde{C}_{0+} and \tilde{C}_{+B} [see Eqs. (52) and (53)] which can change their sign depending on the pulse area (see Fig. 3). However, as is evident from Fig. 3, the relative sign of \tilde{C}_{0+} and \tilde{C}_{+B} does not change. Thus, if at some ω the signs of the GET and EBT spectra are equal (different) then the corresponding nonlinear emissions at this frequency are in (out of) phase for all pulse areas.

3. Biexcitonic coherences

So far we have discussed all elements of the electronic density matrix with one exception, namely, the coherence C_{0B} between the ground and the biexciton state. By using Eq. (43) with $\nu=0$ and $\nu'=B$ we obtain in the strong confinement limit

$$C_{0B}(t) = \theta(t) \bar{C}_{0B} e^{-i\bar{\omega}_B t} G_{\text{GBT}}(t), \quad (60)$$

$$\bar{C}_{0B} = \frac{1}{4} [\cos^2(f_+) - \cos^2(f_-)] e^{i(\varphi_{\sigma^+} + \varphi_{\sigma^-})}, \quad (61)$$

$$G_{\text{GBT}}(t) = g^4(t) s^4(t), \quad (62)$$

where $g(t)$, $s(t)$ are defined in Eqs. (56) and (57).

The amplitude \bar{C}_{0B} vanishes for circular excitations while under linear excitation conditions it reduces to

$$\bar{C}_{0B} = -\sin^2(f/2) e^{2i\varphi/4}. \quad (63)$$

As there is no dipole moment for transitions between $|0\rangle$ and $|B\rangle$ there is no polarization directly associated with the biexcitonic coherence C_{0B} . Nevertheless, it has been shown re-

cently that this coherence is accessible in optical experiments, e.g., by isolating a fully coherent nonlinear signal component in a two-color two-photon absorption experiment with heterodyne detection.⁴⁶ In these experiments the effect of pure dephasing turned out to be negligible which had to be expected, because these measurements were performed with CW lasers. It is known from studies of the excitonic pure dephasing that in the adiabatic limit, which is reached for long pulse durations, pure dephasing disappears due to its non-Markovian nature.⁸⁷ Our theory, in contrast, focuses on the opposite limit of ultrafast excitation, where C_{0B} experiences a nonnegligible pure dephasing. This is demonstrated in Fig. 4 where we have plotted background spectra related to the function $G_{\text{GBT}}(t)$ which, according to Eq. (60), determines the phonon-induced decoherence of the ground state to biexciton transition (GBT). Obviously, the background spectra of GBTs and GETs are of similar shape for weak coupling and at low T . This can be understood again by an expansion at $T=0$ K up to the leading order in the phonon coupling, which yields for $G_{\text{GBT}}(t)$ in Eq. (60)

$$G_{\text{GBT}}(t) \approx \text{const} + 4 \sum_{\xi} |\gamma_{\xi}|^2 e^{-i\omega_{\xi} t}. \quad (64)$$

Apart from the factor four Eq. (64) coincides with the result Eq. (58) for $G_{\text{GET}}(t)$ and explains why the corresponding low-temperature spectra in Fig. 4 have similar shapes but with a roughly four times larger amplitude for the GBT result. The high-temperature behavior is again governed by the term $\propto N_{\xi}$ in the exponential contained in g [see Eq. (60)]. This term has here a four times larger weight than in the GET and EBT cases because g enters in Eq. (62) in the fourth power. Consequently, the GBT spectra do not approach asymptotically the GET and EBT spectra in the high-temperature limit which is clearly reflected in Fig. 4. Instead they are much broader indicating a faster decay in the time domain.

V. CONCLUSIONS

We have discussed the ultrafast dynamics of semiconductor QDs that support excitonic and biexcitonic excitations which are coupled to an arbitrary number of phonon modes. Our main result is the derivation of a recursion formula that allows us to obtain closed form expressions for all elements of the electronic and phononic density matrix for the special case that the QD is excited by a sequence of δ -shaped pulses. Our results are exact within our model and allow us to calculate nonlinear optical signals that are nonperturbative with respect to the carrier-phonon coupling as well as with regard to the carrier-light interaction. In addition, nonequilibrium lattice properties such as coherent phonon amplitudes or nonequilibrium phonon distributions can be calculated with our formulas. The model gives strict results including direct and exchange Coulomb interactions in the limit of strong confinement. For the special case of a single pulse excitation we have worked out explicitly all electronic density matrix elements. Background spectra corresponding to the GET, EBT, and GBT coherences have been calculated for different temperatures and their relation to observable optical signals

has been discussed. The spectra exhibit at low- T asymmetric strongly non-Lorentzian line shapes while they approach symmetrical shapes at high- T values. It turns out that the strong confinement implies a number of special relations which are characteristic for this limit. For example, the amplitudes of GET and EBT polarizations necessarily exhibit identical time evolutions when a strong confinement situation is realized. Interestingly, these transitions still have different real time phases which result in different Fourier representations. While at $T=0$ K GET and GBT spectra are zero below the ZPL this is not true for EBT spectra which assume negative values in this frequency range. It is seen from our more general analytical results that the relations applicable in the strong confinement limit are modified when excitonic and biexcitonic wave functions no longer factorize. Most strikingly, qualitative modifications can be expected from the corresponding changes of the carrier-phonon coupling. Our general formulas have been derived in such a way that they can be directly applied also to this case. However, a quantitative evaluation of such effects is beyond the scope of the present paper. We have also discussed explicitly the pulse area dependence of electronic occupations, phonon amplitudes and densities as well as GET, EBT, and GBT coherences. We find that the period of Rabi rotations is twice as long for the biexciton than for excitons. The generation of nonequilibrium phonons can be strongly enhanced when the biexciton state is occupied. Our analysis of pulse area dependences also reveals that the optically generated nonequilibrium phonons are in general not in a coherent state although in the strong confinement limit their time dependence is correctly described by a product of coherent phonon amplitudes. In view of the growing interest in biexcitonic excitations in semiconductor QDs we believe that our general results, which enable the calculation of nonlinear signals for multipulse excitations, will become helpful for the interpretation of many forthcoming experiments.

ACKNOWLEDGMENTS

The Münster group acknowledges financial support from the Deutsche Forschungsgemeinschaft. A.V. was supported by the Flemish Science Foundation (FWO-VI). Part of this work was supported by the Belgian Science Policy, the FWO-VI, the EU Network of excellence SANDiE and the ESF network: Arrays of quantum dots and Josephson Junctions.

APPENDIX A: DERIVATION OF THE SOLUTION FOR ULTRAFAST PULSES

To solve Eq. (19) we proceed along similar lines as in the two-level case.⁶² However, due to the larger complexity of our present problem a more general strategy is needed. We seek the solution to Eq. (19) in the form

$$\rho_{vv'}(t) = \exp(it\hat{\Lambda}_{vv'}) \tilde{\rho}_{vv'}(t). \quad (A1)$$

The action of the exponential operator in this equation on an arbitrary function $G(\{\alpha_{\xi}\}, \{\beta_{\xi}\}, t)$ is derived in Appendix B and is given by

$$\begin{aligned} \exp(it\hat{\Lambda}_{\nu\nu'}(\{\alpha_{\xi}\},\{\beta_{\xi}\}))G(\{\alpha_{\xi}\},\{\beta_{\xi}\},t) &= G(\{e^{i\omega_{\xi}t}\alpha_{\xi} + (\gamma_{\xi}^{*\prime} - \gamma_{\xi}^{\prime*})(e^{i\omega_{\xi}t} - 1)\},\{e^{-i\omega_{\xi}t}\beta_{\xi} + (\gamma_{\xi}^{\prime} - \gamma_{\xi}^{\prime*})(e^{-i\omega_{\xi}t} - 1)\},t) \\ &\times \exp\left(it(\bar{\omega}_{\nu} - \bar{\omega}_{\nu'})\right) \\ &+ \sum_{\xi} \left\{ \gamma_{\xi}^{\prime*} [(e^{-i\omega_{\xi}t} - 1)(\beta_{\xi} + \gamma_{\xi}^{\prime} - \gamma_{\xi}^{\prime*})] + \gamma_{\xi}^{\prime} [(e^{i\omega_{\xi}t} - 1)(\alpha_{\xi} + \gamma_{\xi}^{*\prime} - \gamma_{\xi}^{\prime*})] \right\}. \quad (\text{A2}) \end{aligned}$$

With the help of Eq. (A2) we are able to evaluate explicitly the generating functions $\rho_{\nu\nu'}(\{\alpha_{\xi}\},\{\beta_{\xi}\},t)$ according to Eq. (A1) once the auxiliary functions $\tilde{\rho}_{\nu\nu'}(\{\alpha_{\xi}\},\{\beta_{\xi}\},t)$ are known. The latter satisfy the equation

$$\begin{aligned} i \exp(it\hat{\Lambda}_{\nu\nu'}) \frac{\partial}{\partial t} \tilde{\rho}_{\nu\nu'} &= \sum_{\bar{\nu}} [\bar{M}_{\nu\bar{\nu}}^* \exp(it\hat{\Lambda}_{\bar{\nu}\nu'}) \tilde{\rho}_{\bar{\nu}\nu'} \\ &- \exp(it\hat{\Lambda}_{\nu\bar{\nu}}) \tilde{\rho}_{\nu\bar{\nu}} \bar{M}_{\bar{\nu}\nu'}^*]. \quad (\text{A3}) \end{aligned}$$

Note, that Eq. (A3) is valid for any pulse shape. It is particularly useful in the ultrafast pulse limit, because according to Eqs. (13) and (15) the matrix \bar{M} on the right-hand side is proportional to the laser amplitudes. Thus, the right-hand side of Eq. (A3) vanishes in between the laser pulses. Consequently, in the limit of an excitation by a sequence of δ functions [see Eq. (24)] $\tilde{\rho}$ has to approach a piecewise constant function of time. However, as noted before in the two level case,⁶² finding the connection between the values of $\tilde{\rho}$ before and after the j th pulse is not a simple amplitude matching problem, because the right-hand side of Eq. (A3) contains in the ultrafast pulse limit products of δ functions and step functions. Such products are not a priori well defined. Instead, they are meaningful only as the result of a limiting procedure, where one has to start with pulses of finite duration and then explicitly go over to the ultrafast limit. This connection will be constructed below by using the following explicit parametrization for the pulse shape during the laser action

$$\delta(t - t_j) = \lim_{\varepsilon \rightarrow 0^+} \begin{cases} \frac{1}{\varepsilon} & \text{for } t_j - \varepsilon/2 < t < t_j + \varepsilon/2, \\ 0 & \text{otherwise.} \end{cases} \quad (\text{A4})$$

We shall work out only the case, where the same pulse shapes are used for both components σ^{\pm} of the j th pulse. Other cases can be treated along the same lines, but will not be considered here. With this restriction, the results discussed below do not depend on the shape of the function that is used to approach the delta function limit (see also the related discussion in Ref. 62).

To proceed, we perform a change of the time variable during the j th pulse according to

$$t(\tau) = \varepsilon\tau + t_j - \varepsilon/2 \quad (\text{A5})$$

such that $\tau=0$ corresponds to the beginning and $\tau=1$ to the end of the j th pulse. By rewriting Eq. (A3) in terms of the scaled time variable τ and then taking the limit $\varepsilon \rightarrow 0^+$ in the resulting equation we obtain

$$\frac{\partial}{\partial \tau} \tilde{\rho}_{\nu\nu'}^{(j)} = -i \sum_{\bar{\nu}} (Q_{\nu\bar{\nu}}^{(j)} \tilde{\rho}_{\bar{\nu}\nu'}^{(j)} - \tilde{\rho}_{\nu\bar{\nu}}^{(j)} Q_{\bar{\nu}\nu'}^{(j)}). \quad (\text{A6})$$

Here, we have defined

$$Q^{(j)} \equiv S^{-1} M^{(j)} S, \quad (\text{A7})$$

where S is the 4×4 transformation matrix introduced in Eq. (14) and $M^{(j)}$ is a matrix describing the pulse characteristics of the j th pulse. It can be constructed by replacing the entries Ω_{σ} in the definition of the matrix M [see Eq. (15)] by $f_{j\sigma} e^{-i\varphi_{j\sigma}/2}$. In addition we have set

$$\tilde{\rho}_{\nu\nu'}^{(j)}(\tau) = \exp(it_j \hat{\Lambda}_{\nu\nu'}) \tilde{\rho}_{\nu\nu'}^{(j)}(\tau), \quad (\text{A8})$$

where $\tilde{\rho}_{\nu\nu'}^{(j)}(\tau)$ represents $\tilde{\rho}_{\nu\nu'}(\tau)$ as a function of τ during the j th pulse in the limit $\varepsilon \rightarrow 0^+$. Finally, in the derivation of Eq. (A6) we have used that $\lim_{\varepsilon \rightarrow 0^+} t(\tau) = t_j$ and thus the operator $\exp[it(\tau)\hat{\Lambda}_{\nu\nu'}]$ becomes independent of τ . This is the mathematical manifestation of the physical fact that during an excitation with ultrafast pulses the phonon system cannot noticeably change its state. The solution of Eq. (A6) is found as

$$\tilde{\rho}_{\nu\nu'}^{(j)}(\tau) = \exp(-i\tau Q^{(j)}) \tilde{\rho}_{\nu\nu'}^{(j)}(\tau=0) \exp(i\tau Q^{(j)}), \quad (\text{A9})$$

because $Q^{(j)}$ does not depend on τ . The matrix exponent in Eq. (A9) is obtained by expressing $Q^{(j)}$ in the form

$$Q^{(j)} = S^{-1} U_j^{-1} D_j U_j S, \quad (\text{A10})$$

where S is defined by Eq. (14), D_j is a diagonal matrix with the eigenvalues of $M^{(j)}$ on its diagonal

$$D_j = \begin{pmatrix} f_{j+} & & & \\ & f_{j-} & & \\ & & -f_{j+} & \\ & & & -f_{j-} \end{pmatrix} \quad (\text{A11})$$

with

$$f_{j\pm} = \frac{1}{2}(f_{j\sigma^+} \pm f_{j\sigma^-}) \quad (\text{A12})$$

and U_j is the matrix formed by the corresponding eigenvectors

$$U_j = \frac{1}{2} \begin{pmatrix} 1 & 1 & 1 & 1 \\ 1 & 1 & -1 & -1 \\ 1 & -1 & -1 & 1 \\ 1 & -1 & 1 & -1 \end{pmatrix} \begin{pmatrix} 1 \\ e^{i\varphi_{j\sigma^+}} \\ e^{i\varphi_{j\sigma^-}} \\ e^{i(\varphi_{j\sigma^+} + \varphi_{j\sigma^-})} \end{pmatrix}. \quad (\text{A13})$$

Writing the matrix exponent as

$$\exp(\pm i\tau Q^{(j)}) = S^{-1} U_j^{-1} \exp(\pm i\tau D_j) U_j S, \quad (\text{A14})$$

reduces its evaluation to the elementary task of taking the exponent of the diagonal matrix $\pm i\tau D_j$.

Recalling that $\tau=0$ ($\tau=1$) describes the situation immediately before (after) the j th pulse we obtain by combining Eqs. (A1), (A8), and (A9) the complete solution for times $t_j < t < t_{j+1}$ in form given by Eq. (25).

APPENDIX B: EVALUATION OF EXPONENTIAL OPERATOR ACTIONS

Here we shall determine explicitly the action of exponential operators where the operator $\hat{\Lambda}_{\nu\nu'}(\{\alpha_{\xi_j}\}, \{\beta_{\xi_j}\})$ defined in Eq. (20) appears in the exponent. First we note that according to Eq. (20) the operator $\hat{\Lambda}_{\nu\nu'}(\{\alpha_{\xi_j}\}, \{\beta_{\xi_j}\})$ is, apart from a constant term, the sum of operators $\hat{L}(\omega, \kappa, \lambda, x)$ that act on different variables x and thus commute. Here, x stands either for $x=\alpha_{\xi}$ or $x=\beta_{\xi}$. Consequently, taking $\hat{\Lambda}_{\nu\nu'}(\{\alpha_{\xi_j}\}, \{\beta_{\xi_j}\})$ in the exponent results in operator products where each factor \hat{F}_x acts on a different variable x and has the form

$$\hat{F}_x \equiv \exp[\hat{L}(\omega, \kappa, \lambda, x)] = \exp(\omega x \partial_x + \kappa \partial_x + \lambda x) \quad (\text{B1})$$

with suitably chosen parameters ω , κ , and λ . Our task is thus to evaluate the action of \hat{F}_x on an arbitrary function of x . To this end we start by recalling the well known operator identities⁸⁸

$$e^{-\hat{B}} e^{\hat{A}} e^{\hat{B}} = \exp(e^{-\hat{B}} \hat{A} e^{\hat{B}}), \quad (\text{B2})$$

$$e^{-\hat{B}} \hat{A} e^{\hat{B}} = \hat{A} + [\hat{A}, \hat{B}] + \frac{1}{2!} [[\hat{A}, \hat{B}], \hat{B}] + \dots, \quad (\text{B3})$$

where $[\dots]$ denotes the commutator. Choosing $\hat{A} = \omega x \partial_x$ and $\hat{B} = (\lambda/\omega)x$, we obtain from Eqs. (B2) and (B3)

$$\exp\left(\frac{-\lambda x}{\omega}\right) \exp(\omega x \partial_x) \exp\left(\frac{\lambda x}{\omega}\right) = \exp(\omega x \partial_x + \lambda x). \quad (\text{B4})$$

Next we set $\hat{A} = \omega x \partial_x + \lambda x$ and $\hat{B} = -(\kappa/\omega) \partial_x$ which according to Eqs. (B2) and (B3) results in

$$\begin{aligned} & \exp\left(\frac{\kappa}{\omega} \partial_x\right) \exp(\omega x \partial_x + \lambda x) \exp\left(\frac{-\kappa}{\omega} \partial_x\right) \\ &= \exp\left(\omega x \partial_x + \lambda x + \kappa \partial_x + \frac{\kappa \lambda}{\omega}\right). \end{aligned} \quad (\text{B5})$$

Combining Eqs. (B4) and (B5) we obtain

$$\begin{aligned} & \exp(\omega x \partial_x + \lambda x + \kappa \partial_x) \\ &= \exp\left(\frac{-\kappa \lambda}{\omega}\right) \exp\left(\frac{\kappa}{\omega} \partial_x\right) \exp\left(\frac{-\lambda}{\omega} x\right) \\ & \quad \times \exp(\omega x \partial_x) \exp\left(\frac{\lambda}{\omega} x\right) \exp\left(\frac{-\kappa}{\omega} \partial_x\right). \end{aligned} \quad (\text{B6})$$

Now we will exploit the fact that the action of the exponential operators on the right-hand side of Eq. (B6) on an arbitrary function $G(x)$ is given by

$$\exp(\kappa \partial_x) G(x) = G(x + \kappa), \quad (\text{B7a})$$

$$\exp(\omega x \partial_x) G(x) = G(x e^\omega). \quad (\text{B7b})$$

These identities can be established simply by expanding both the function $G(x)$ and the exponential operators into their Taylor series. The sought action of \hat{F}_x on an arbitrary function $G(x)$ is finally found by combining Eq. (B6) with Eqs. (B7)

$$\begin{aligned} \hat{F}_x G(x) &= \exp(\omega x \partial_x + \kappa \partial_x + \lambda x) G(x) \\ &= G\left(e^\omega x + \frac{\kappa}{\omega}(e^\omega - 1)\right) \\ & \quad \times \exp\left\{\frac{\lambda}{\omega} \left[(e^\omega - 1)\left(x + \frac{\kappa}{\omega}\right) - \kappa\right]\right\}. \end{aligned} \quad (\text{B8})$$

The action of $\exp[it\hat{\Lambda}_{\nu\nu'}(\{\alpha_{\xi_j}\}, \{\beta_{\xi_j}\})]$ follows immediately from the identity Eq. (B8) by identifying the parameters ω , κ , and λ for each operator factor corresponding to a specific choice of either $x=\alpha_{\xi}$ or $x=\beta_{\xi}$. The result is given explicitly by Eq. (A2).

¹U. Woggon, *Optical Properties of Semiconductors Quantum Dots*, Vol. 136 of *Springer Tracts in Modern Physics* (Springer, Berlin, 1997).

²D. Bimberg, M. Grundmann, and N. N. Ledentsov, *Quantum Dot Heterostructures* (Wiley, Chichester, 1998).

³M. Bayer, T. Gutbrod, A. Forchel, V. D. Kulakovskii, A. Gorbunov, M. Michel, R. Steffen, and K. H. Wang, *Phys. Rev. B* **58**, 4740 (1998).

⁴M. Bayer, O. Stern, P. Hawrylak, S. Fafard, and A. Forchel, *Nature* (London) **405**, 923 (2000).

⁵R. Rinaldi, S. Antonaci, M. DeVittorio, R. Cingolani, U. Hohenester, E. Molinari, H. Lipsanen, and J. Tulkki, *Phys. Rev. B* **62**, 1592 (2000).

⁶S. V. Nair and Y. Masumoto, *Phys. Status Solidi B* **224**, 739 (2001).

⁷P. Borri, W. Langbein, S. Schneider, U. Woggon, R. L. Sellin, D.

- Ouyang, and D. Bimberg, Phys. Rev. Lett. **89**, 187401 (2002).
- ⁸L. Besombes, K. Kheng, L. Marsal, and H. Mariette, Phys. Rev. B **65**, 121314(R) (2002).
- ⁹L. Jacak, P. Hawrylak, and A. Wójs, *Quantum Dots* (Springer, Berlin, 1998).
- ¹⁰M. Bayer, A. Kuther, A. Forchel, A. Gorbunov, V. B. Timofeev, F. Schäfer, J. P. Reithmaier, T. L. Reinecke, and S. N. Walck, Phys. Rev. Lett. **82**, 1748 (1999).
- ¹¹U. Woggon, F. Gindele, O. Wind, and C. Klingshirn, Phys. Rev. B **54**, 1506 (1996).
- ¹²L. Besombes, K. Kheng, L. Marsal, and H. Mariette, Phys. Rev. B **63**, 155307 (2001).
- ¹³J. J. Finley, D. J. Mowbray, M. S. Skolnick, A. D. Ashmore, C. Baker, A. F. G. Monte, and M. Hopkinson, Phys. Rev. B **66**, 153316 (2002).
- ¹⁴M. Bayer, G. Ortner, O. Stern, A. Kuther, A. A. Gorbunov, A. Forchel, P. Hawrylak, S. Fafard, K. Hinzer, T. L. Reinicke, and S. N. Walck, Phys. Rev. B **65**, 195315 (2002).
- ¹⁵M. Bayer and A. Forchel, Phys. Rev. B **65**, 041308(R) (2002).
- ¹⁶A. Högele, S. Seidl, M. Kroner, K. Karrai, R. J. Warburton, B. D. Gerardot, and P. M. Petroff, Phys. Rev. Lett. **93**, 217401 (2004).
- ¹⁷B. Urbaszek, E. J. McGhee, M. Krüger, R. J. Warburton, K. Karrai, T. Amand, B. D. Gerardot, P. M. Petroff, and J. M. Garcia, Phys. Rev. B **69**, 035304 (2004).
- ¹⁸W. Langbein, P. Borri, U. Woggon, V. Stavarache, D. Reuter, and A. D. Wieck, Phys. Rev. B **70**, 033301 (2004).
- ¹⁹A. Kuther, M. Bayer, A. Forchel, A. Gorbunov, V. B. Timofeev, F. Schäfer, and J. P. Reithmaier, Phys. Rev. B **58**, R7508 (1998).
- ²⁰F. Gindele, U. Woggon, W. Langbein, J. M. Hvam, K. Leonardi, D. Hommel, and H. Selke, Phys. Rev. B **60**, 8773 (1999).
- ²¹F. Gindele, K. Hild, W. Langbein, and U. Woggon, Phys. Rev. B **60**, R2157 (1999).
- ²²U. Hohenester, F. Rossi, and E. Molinari, Physica B **272**, 1 (1999).
- ²³J. J. Finley, P. W. Fry, A. D. Ashmore, A. Lemaître, A. I. Tartakovskii, R. Oulton, D. J. Mowbray, M. S. Skolnick, M. Hopkinson, P. D. Buckle, and P. A. Maksym, Phys. Rev. B **63**, 161305(R) (2001).
- ²⁴K. Hinzer, P. Hawrylak, M. Korkusinski, S. Fafard, M. Bayer, O. Stern, A. Gorbunov, and A. Forchel, Phys. Rev. B **63**, 075314 (2001).
- ²⁵U. Hohenester, Phys. Rev. B **66**, 245323 (2002).
- ²⁶V. Zwiller, P. Jonsson, H. Blom, S. Jeppesen, M.-E. Pistol, L. Samuelson, A. A. Katznelson, E. Y. Kotelnikov, V. Evtikhiev, and G. Björk, Phys. Rev. A **66**, 053814 (2002).
- ²⁷G. Bacher, R. Weigand, J. Seufert, V. D. Kulakovskii, N. A. Gippius, A. Forchel, K. Leonardi, and D. Hommel, Phys. Rev. Lett. **83**, 4417 (1999).
- ²⁸V. D. Kulakovskii, K. Babocsi, M. Schmitt, N. A. Gippius, and W. Kiefer, Phys. Rev. B **67**, 113303 (2003).
- ²⁹H. Gotoh, H. Kamada, T. Saitoh, H. Ando, and J. Temmyo, Phys. Rev. B **69**, 155328 (2004).
- ³⁰E. Peter, J. Hours, P. Senellart, A. Vasanelli, A. Cavanna, J. Bloch, and J. M. Gérard, Phys. Rev. B **69**, 041307(R) (2004).
- ³¹U. Hohenester, G. Goldoni, and E. Molinari, Appl. Phys. Lett. **84**, 3963 (2004).
- ³²B. Patton, W. Langbein, and U. Woggon, Phys. Rev. B **68**, 125316 (2003).
- ³³A. S. Lenihan, M. V. Gurudev Dutt, D. G. Steel, S. Ghosh, and P. Bhattacharya, Phys. Rev. B **69**, 045306 (2004).
- ³⁴T. Takagahara, Phys. Rev. B **39**, 10 206 (1989).
- ³⁵L. Bányai, Phys. Rev. B **39**, 8022 (1989).
- ³⁶G. W. Bryant, Phys. Rev. B **41**, 1243 (1990).
- ³⁷Y. Z. Hu, S. W. Koch, M. Lindberg, N. Peyghambarian, E. L. Pollock, and F. F. Abraham, Phys. Rev. Lett. **64**, 1805 (1990).
- ³⁸Y. Z. Hu, M. Lindberg, and S. W. Koch, Phys. Rev. B **42**, 1713 (1990).
- ³⁹O. Heller, P. Lelong, and G. Bastard, Phys. Rev. B **56**, 4702 (1997).
- ⁴⁰U. Woggon, K. Hild, F. Gindele, W. Langbein, M. Hetterich, M. Grün, and C. Klingshirn, Phys. Rev. B **61**, 12 632 (2000).
- ⁴¹O. Stier, A. Schliwa, R. Heitz, M. Grundmann, and D. Bimberg, Phys. Status Solidi B **224**, 115 (2001).
- ⁴²R.-H. Xie, G. W. Bryant, S. Lee, and W. Jaskólski, Phys. Rev. B **65**, 235306 (2002).
- ⁴³W. Langbein, P. Borri, U. Woggon, V. Stavarache, D. Reuter, and A. D. Wieck, Phys. Rev. B **69**, 161301(R) (2004).
- ⁴⁴F. Findeis, A. Zrenner, G. Böhm, and G. Abstreiter, Phys. Rev. B **61**, R10 579 (2000).
- ⁴⁵F. Findeis, A. Zrenner, G. Böhm, and G. Abstreiter, Phys. Status Solidi B **224**, 337 (2001).
- ⁴⁶G. Chen, T. H. Stievater, E. T. Batteh, X. Li, D. G. Steel, D. D. Gammon, D. S. Katzer, D. Park, and L. J. Sham, Phys. Rev. Lett. **88**, 117901 (2002).
- ⁴⁷O. Benson, C. Santori, M. Pelton, and Y. Yamamoto, Phys. Rev. Lett. **84**, 2513 (2000).
- ⁴⁸O. Gywat, G. Burkard, and D. Loss, Phys. Rev. B **65**, 205329 (2002).
- ⁴⁹V. Klimov, S. Hunsche, and H. Kurz, Phys. Rev. B **50**, 8110 (1994).
- ⁵⁰T. H. Stievater, X. Li, D. G. Steel, D. Gammon, D. S. Katzer, and D. Park, Phys. Rev. B **65**, 205319 (2002).
- ⁵¹P. Borri, W. Langbein, S. Schneider, U. Woggon, R. L. Sellin, D. Ouyang, and D. Bimberg, Phys. Rev. Lett. **87**, 157401 (2001).
- ⁵²A. E. Colonna, X. Yang, and G. D. Scholes, Phys. Status Solidi B **242**, 990 (2005).
- ⁵³F. Troiani, U. Hohenester, and E. Molinari, Phys. Rev. B **62**, R2263 (2000).
- ⁵⁴P. Chen, C. Piermarocchi, and L. J. Sham, Phys. Rev. Lett. **87**, 067401 (2001).
- ⁵⁵C. Piermarocchi, P. Chen, Y. S. Dale, and L. J. Sham, Phys. Rev. B **65**, 075307 (2002).
- ⁵⁶E. Biolatti, I. D'Amico, P. Zanardi, and F. Rossi, Phys. Rev. B **65**, 075306 (2002).
- ⁵⁷X. Q. Li, Y. W. Wu, D. Steel, D. Gammon, T. H. Stievater, D. S. Katzer, D. Park, C. Piermarocchi, and L. J. Sham, Science **301**, 809 (2003).
- ⁵⁸X. D. Fan, T. Takagahara, J. E. Cunningham, and H. L. Wang, Solid State Commun. **108**, 857 (1998).
- ⁵⁹P. Borri, W. Langbein, J. Mørk, J. M. Hvam, F. Heinrichsdorff, M.-H. Mao, and D. Bimberg, Phys. Rev. B **60**, 7784 (1999).
- ⁶⁰D. Birkedal, K. Leosson, and J. M. Hvam, Phys. Rev. Lett. **87**, 227401 (2001).
- ⁶¹B. Krummheuer, V. M. Axt, and T. Kuhn, Phys. Rev. B **65**, 195313 (2002).
- ⁶²A. Vagov, V. M. Axt, and T. Kuhn, Phys. Rev. B **66**, 165312 (2002).
- ⁶³A. Vagov, V. M. Axt, and T. Kuhn, Phys. Rev. B **67**, 115338 (2003).
- ⁶⁴A. Vagov, V. M. Axt, T. Kuhn, W. Langbein, P. Borri, and U.

- Woggon, Phys. Rev. B **70**, 201305(R) (2004).
- ⁶⁵L. Jacak, J. Krasnyj, D. Jacak, and P. Machnikowski, Phys. Rev. B **65**, 113305 (2002).
- ⁶⁶T. Itakura and Y. Tokura, Phys. Rev. B **67**, 195320 (2003).
- ⁶⁷U. Hohenester and G. Stadler, Phys. Rev. Lett. **92**, 196801 (2004).
- ⁶⁸V. M. Axt, P. Machnikowski, and T. Kuhn, Phys. Rev. B **71**, 155305 (2005).
- ⁶⁹G. D. Mahan, *Many-Particle Physics*, 2nd ed. (Plenum Press, New York, 1990).
- ⁷⁰K. Huang and A. Rhys, Proc. R. Soc. London, Ser. A **204**, 406 (1950).
- ⁷¹C. B. Duke and G. Mahan, Phys. Rev. **139**, A1965 (1965).
- ⁷²P. Borri, W. Langbein, S. Schneider, U. Woggon, R. L. Sellin, D. Ouyang, and D. Bimberg, Phys. Rev. B **66**, 081306(R) (2002).
- ⁷³T. Takagahara, Phys. Rev. B **47**, 4569 (1993).
- ⁷⁴T. Takagahara, Phys. Rev. B **62**, 16 840 (2000).
- ⁷⁵B. W. Lovett, J. H. Reina, A. Nazir, and G. A. Briggs, Phys. Rev. B **68**, 205319 (2003).
- ⁷⁶F. Rossi and T. Kuhn, Rev. Mod. Phys. **74**, 895 (2002).
- ⁷⁷D. Gammon, E. S. Snow, B. V. Shanabrook, D. S. Katzer, and D. Park, Phys. Rev. Lett. **76**, 3005 (1996).
- ⁷⁸P. Borri, W. Langbein, S. Schneider, U. Woggon, R. L. Sellin, D. Ouyang, and D. Bimberg, Phys. Status Solidi B **233**, 391 (2002).
- ⁷⁹M. Herbst, M. Glanemann, V. M. Axt, and T. Kuhn, Phys. Rev. B **67**, 195305 (2003).
- ⁸⁰A. Vagov, V. M. Axt, and T. Kuhn, Physica E (Amsterdam) **17**, 11 (2003).
- ⁸¹J. J. Baumberg, D. A. Williams, and K. Köhler, Phys. Rev. Lett. **78**, 3358 (1997).
- ⁸²B. Krummheuer, A. Vagov, V. M. Axt, T. Kuhn, I. D'Amico, and F. Rossi, Semicond. Sci. Technol. **19**, S31 (2004).
- ⁸³P. Hawker, A. J. Kent, and M. Henini, Appl. Phys. Lett. **75**, 3832 (1999).
- ⁸⁴R. Bellingham, A. J. Kent, A. V. Akimov, and M. Henini, Phys. Status Solidi B **224**, 659 (2001).
- ⁸⁵V. M. Axt, B. Krummheuer, A. Vagov, and T. Kuhn, Phys. Status Solidi B **238**, 581 (2003).
- ⁸⁶B. Krummheuer, V. M. Axt, T. Kuhn, I. D'Amico, and F. Rossi, Phys. Rev. B **71**, 235329 (2005).
- ⁸⁷R. Alicki, M. Horodecki, P. Horodecki, R. Horodecki, L. Jacak, and P. Machnikowski, Phys. Rev. A **70**, 010501(R) (2004).
- ⁸⁸L. Mandel and E. Wolf, *Optical Coherence and Quantum Optics* (Cambridge University Press, Cambridge, 1995).